Published in final edited form as:
Messenger (Los Angel). 2015 June ; 4(1): 104–111. doi:10.1166/msr.2015.1045.

Calcium Signalling Triggered by NAADP in T Cells Determines Cell Shape and Motility During Immune Synapse Formation

Merle Nebel[1], **Bo Zhang**[3], **Francesca Odoardi**[4], **Alexander Flügel**[4], **Barry V. L. Potter**[3], and **Andreas H. Guse**[1,2,*]

[1]The Calcium Signalling Group, Department of Biochemistry and Signal Transduction, University Medical Centre Hamburg-Eppendorf, Martinistrasse 52, 20246 Hamburg, Germany

[2]Department of Biochemistry and Molecular Cell Biology, University Medical Centre Hamburg-Eppendorf, Martinistrasse 52, 20246 Hamburg, Germany

[3]Wolfson Laboratory of Medicinal Chemistry, Department of Pharmacy and Pharmacology, University of Bath, Claverton Down, Bath BA2 7AY, UK

[4]Institute for Multiple Sclerosis Research, Department of Neuroimmunology, Gemeinnützige Hertie-Stiftung and University Medical Centre Göttingen, 37073 Göttingen, Germany

Abstract

Nicotinic acid adenine dinucleotide phosphate (NAADP) has been implicated as an initial Ca^{2+} trigger in T cell Ca^{2+} signalling, but its role in formation of the immune synapse in $CD4^+$ effector T cells has not been analysed. $CD4^+$ T cells are activated by the interaction with peptide-MHCII complexes on the surface of antigen-presenting cells. Establishing a two-cell system including primary rat $CD4^+$ T cells specific for myelin basic protein and rat astrocytes enabled us to mirror this activation process *in vitro* and to analyse Ca^{2+} signalling, cell shape changes and motility in T cells during formation and maintenance of the immune synapse. After immune synapse formation, T cells showed strong, antigen-dependent increases in free cytosolic calcium concentration ($[Ca^{2+}]_i$). Analysis of cell shape and motility revealed rounding and immobilization of T cells depending on the amplitude of the Ca^{2+} signal. NAADP-antagonist BZ194 effectively blocked Ca^{2+} signals in T cells evoked by the interaction with antigen-presenting astrocytes. BZ194 reduced the percentage of T cells showing high Ca^{2+} signals thereby supporting the proposed trigger function of NAADP for global Ca^{2+} signalling. Taken together, the NAADP signalling pathway is further confirmed as a promising target for specific pharmacological intervention to modulate T cell activation.

Keywords

NAADP; T Cell Activation; Cytoskeleton; Ca^{2+} Signalling; Live Cell Imaging

*Author to whom correspondence should be addressed. guse@uke.de.

Europe PMC Funders Author Manuscripts

Introduction

Ca^{2+} signalling plays an essential role in early T cell activation. Ligation of the T cell receptor/CD3 complex (TCR/CD3) results in signal transduction across the plasma membrane followed by formation of the second messengers NAADP (Gasser et al., 2006), D-*myo*-inositol 1,4,5-trisphosphate (IP_3; Guse et al., 1995), and cyclic ADP-ribose (cADPR; Guse et al., 1999) in a specific temporal sequence. Among these second messengers, NAADP is unique since it acts at effective concentrations in the nanomolar range (Lee and Aarhus, 1995) and initiates global Ca^{2+} signalling as a trigger [reviewed in Guse and Lee (2008)]. Indeed, NAADP is the most potent Ca^{2+}-releasing second messenger known so far, present in mammals, invertebrates and plants [reviewed in Lee, 2012; Morgan et al., 2011].

Though receptor-evoked formation of NAADP has been described in several cell systems (Gasser et al., 2006; Masgrau et al., 2003; Yamasaki et al., 2005; Kim et al., 2008; Barceló-Torns et al., 2011; Lewis et al., 2012) both enzymes involved in NAADP metabolism (Aarhus et al., 1995; Soares et al., 2007; Cosker et al., 2010; Schmid et al., 2011) as well as the NAADP receptor and/or target channel (Mojzisová et al., 2001; Hohenegger et al., 2002; Gerasimenko et al., 2003, 2006; Dammermann et al., 2009; Zhang and Li, 2007; Zhang et al., 2009; Calcraft et al., 2009; Brailoiu et al., 2009; Ogunbayo et al., 2011; Yamaguchi et al., 2011; Wang et al., 2012) are still a matter of debate. As a unifying hypothesis for NAADP's mode of action, we recently proposed that it might first bind to cytosolic NAADP binding proteins (Lin-Moshier et al., 2012; Walseth et al., 2012); then NAADP bound to its binding protein might activate different channel types, depending on cell type, extracellular stimulus and perhaps other conditions (Guse, 2012).

However, several studies support a trigger function of NAADP for global Ca^{2+} signalling. In both pancreatic acinar and islet cells NAADP rapidly increased after stimulation and preceded an increase in cADPR concentration (Yamasaki et al., 2005; Kim et al., 2008). Jurkat T-lymphocytes stimulated via TCR/CD3 show very similar results since NAADP rapidly increased within seconds and likely initiated local Ca^{2+} signals in the so-called pacemaker phase of Ca^{2+} signalling (Gasser et al., 2006; Kunerth et al., 2004). Infusion or microinjection experiments in Jurkat T cells showed NAADP evoked Ca^{2+} signals in restricted trigger zones (Dammermann and Guse, 2005).

While scanning their environment, the cytoskeleton of T cells undergoes permanent changes allowing for both integrin-dependent and -independent types of motion [reviewed in Krummel and Cahalan, 2010]. While integrin-independent motility is more rapid and dependent on myosin, velocity in the integrin-dependent mode is reduced and thus more cell–cell contacts are possible. The situation changes as soon as antigenic peptide in MHCII context is recognized. Then, T cells may either intensify scanning the APC while motility is reduced, but not fully abrogated. Another possibility is formation of the Immune synapse (IS) with rounding of T cells and full stop of motility (Donnadieu et al., 1994). The latter is accompanied by ongoing polymerization and inward streaming of actin into the IS (Kaizuka et al., 2007).

Obviously, velocity of T cell motility depends on integrin interactions, but it is less clear what mechanisms underlie the step from intense scanning at low velocity to T cell rounding and full IS formation. Ca^{2+} signalling has been implicated in this process and it has been shown that several proteins involved, including proteins involved in Ca^{2+} release activated Ca^{2+} entry, such as Orai1 and Stim1, or the potassium channels $K_{Ca}3.1$, and $K_V1.3$, co-localize at the IS [reviewed in (Krummel and Cahalan, 2010)].

In this study we used primary rat MBP-specific T cells and the rat astrocyte cell line F10 (in the following termed “astrocytes”) as APC to analyse the role of NAADP during IS formation. Since we previously demonstrated rapid formation of NAADP, we hypothesized that NAADP mediated local Ca^{2+} release might regulate early processes of IS formation, e.g., the step from slowly scanning to immotile rounded T cells. Thus, we recorded in parallel changes in $[Ca^{2+}]_i$ cellular shape, and motility of the T cells following contact to astrocytes. The role of NAADP was assessed by blocking NAADP action using the recently validated small-molecule NAADP antagonist BZ194 (Dammermann et al., 2009; Cordiglieri et al., 2010).

Experimental Details

Materials

Fura-2/AM was purchased from Calbiochem. DMSO and probenecid were supplied by Sigma. Fibronectin was obtained from Invitrogen. BZ194 was synthesized as described (Dammermann et al., 2009).

Antigens

Antigen specific T cell clones were specific for guinea pig myelin basic protein (MBP). MBP was purified from guinea pig brains as reported (Eylar et al., 1979).

Generation and Culturing of T Cells

Rat antigen-specific T cell clones were obtained from lymph node preparations of Lewis rats immunized with MBP. Stimulation, expansion and culture of specific rat T cells were conducted under conditions as described (Flügel et al., 1999).

Analysis of $[Ca^{2+}]_i$, Shape and Motility

Rat T_{MBP} cells were loaded with Fura-2/AM as described (Guse et al., 1993) and kept in the dark at ~15 °C until use. Rat F10 astrocytes with up-regulated MHC II (after 48 h-incubation with T cell-blast-conditioned medium) were cultured on μ-slides 8 well (ibidi, Martinsried, Germany) on fibronectin and pulsed or not with MBP (10 μg/ml, 2 hours). Ratiometric Ca^{2+} imaging was performed as described recently (Berg et al., 2000). We used an Improvision imaging system (Tübingen, Germany) built around the Leica microscope at 40-fold magnification. Illumination at 340 and 380 nm was carried out using a monochromator system (Polychromator IV, TILL Photonics, Gräfelfing, Germany). Images were taken with a grayscale CCD camera (type C4742-95-12ER; Hamamatsu, Enfield, United Kingdom) operated in 8-bit mode. The spatial resolution was 510 × 672 pixels. The acquisition rate was ~1 ratio in 10 seconds. Raw data images were stored on a hard disk. The images were

used to construct ratio images (340/380). Finally, ratio values were converted to Ca^{2+} concentrations by external calibration. To reduce noise, ratio images were subjected to median filter (3 × 3) as described previously.[42] Data processing was performed using Openlab software (Improvision, Tübingen, Germany). Image J software (freeware, provided by Wayne Rasband, NIH) was used to evaluate cell shape and velocity. Shape index is defined as $P^2/4\pi S$ (P: perimeter; S: surface of the cell; Donnadieu et al., 1994).

Results

Fura2-loaded T_{MBP} cells were added to a monolayer of astrocytes and fluorescence images were used to monitor $[Ca^{2+}]_i$ of the T cells. For every tenth fluorescence image a transmitted light image was obtained to follow the interaction of T cells with astrocytes. Time-point zero is defined as first visible contact between a T cell and an astrocyte, as assessed by bright field microscopy.

In the absence of the specific antigen, the T_{MBP} cells remained predominantly quiescent without much alteration of $[Ca^{2+}]_i$ (Fig. 1(A), images and upper panel). Within the first ten minutes after contact to the astrocytes, we defined high- and low-responder T cells showing an increase in $[Ca^{2+}]_i \geq 300$ nM (high-responder) or < 300 nM (low-responder). Over 90% of the T cells stayed below a $[Ca^{2+}]_i$ of 300 nM in the absence of MBP (Fig. 1(A), images and upper panel). Although T cells added to astrocytes were more or less spherical, their shape changed constantly during the experiment. Several pseudopodia reached out indicating a continuous search for specific antigen. This process was quantitatively analysed using the shape index, where an ideal circular shape corresponds to a shape index of 1 and any deviation increases this value (Fig. 1(A) middle panel (Donnadieu et al., 1994); for details see Methods Section). In addition, T cells were still mobile and tended to move around rather than staying in contact with one astrocyte (Fig. 1(A) lower panel). In contrast, when T_{MBP} cells recognized MBP-pulsed astrocytes, within tens of seconds the majority of the T_{MBP} cells displayed high $[Ca^{2+}]_i$ responses (Fig. 1(B), images and upper panel). These high-responder T_{MBP} cells started to round up immediately after onset of the Ca^{2+}-signal (Fig. 1(B), middle panel) and showed strong immobilization (Fig. 1(B), lower panel). Immobilization led to a stable interaction with astrocytes for the duration of the measurement indicating full formation of IS.

Although cellular characteristics such as shape and motility are individual parameters with quite high differences between individual T cells, grouping the T cells into high- and low-responders in terms of Ca^{2+} signalling and averaging the single cell data revealed marked differences between the two groups (Fig. 2). In the absence of MBP 10 out of 12 T_{MBP} cells showed an increase in $[Ca^{2+}]_i < 300$ nM in the first ten minutes. This majority of cells, the typical low-responder T_{MBP} cells, were low in $[Ca^{2+}]_i$ (Fig. 2(A), upper panel), displayed an increased shape index over time (Fig. 2(A), middle panel), and showed motilities between 2 and 3 μm/min on average (Fig. 2(A), lower panel). Upon presentation of MBP by the astrocytes, the typical high-responder T_{MBP} cells were in the majority (Fig. 2(B), upper panel). Further, cellular rounding as judged by a drop in cell shape upon IS formation was observed (Fig. 2(B), middle panel). The T_{MBP} cells were virtually “caught” by the astrocytes since also the motility decreased in parallel to cellular rounding (Fig. 2(B), lower panel).

Although, low-responders in the presence of antigen started to immobilize, too, this arrest was not as strong as for the high-responders.

Having this cellular assay with three read-outs at hand, the role of NAADP in formation of the IS was analysed. Recently, we showed that the small molecular NAADP antagonist BZ194 blocks local and global Ca^{2+} signalling evoked by NAADP, but not by cADPR, IP_3 or by activation of capacitative Ca^{2+} entry evoked by thapsigargin (Dammermann et al., 2009). Here, we demonstrate that BZ194 decreases the overall Ca^{2+}-response of T_{MBP} cells by reducing the percentage of high-responder cells (Fig. 3, pie diagrams and upper panel). Upon preincubation with BZ194, 56% of the T cells showed a low Ca^{2+} response after contact to MBP peptide-presenting astrocytes, whereas in vehicle controls only 30% of T cells were low-responders (Fig. 3, pie diagrams). In this series of experiments, without antigen none of the T cells showed an increase in $[Ca^{2+}]_i > 300$ nM in the first ten minutes after contact (Fig. 3, pie diagrams and A, upper panel). Although BZ194 shifted the percentage of high-responders from 70% down to 44% (Fig. 3, pie diagrams), it is important to note that there was no further influence of BZ194 on the extent of immobilization and rounding up in BZ194 treated high responder T_{MBP} cells. Typically, T_{MBP} cells showed stronger immobilization and rounding up the higher $[Ca^{2+}]_i$ rose (Fig. 3(B)). The same was observed for T_{MBP} cells pre-incubated with BZ194 (Fig. 3(C)). Although less of these T_{MBP} cells showed high Ca^{2+} responses in the presence of MBP, they were neither impaired regarding their shape change nor in motility. These high-responder T_{MBP} cells, though diminished in number, were still capable to round up and slow down to approx. 1 μm/min during Ca^{2+} signalling (Fig. 3(C)). In contrast, the majority of BZ194-treated low-responding T_{MBP} cells extended several pseudopodia and moved around on top of the astrocyte layer (Fig. 3(C)). This indicates that BZ194 is able to block Ca^{2+} signalling without affecting other essential cellular processes like shape changes due to cytoskeletal rearrangements and motility.

Discussion

Upon IS formation between CD4+ T_{MBP} cells and astrocytes we observed (i) rapid T cell Ca^{2+} signalling, and (ii) concomitant decrease in cell shape index (rounding) and motility. While the percentage of high-responder T_{MBP} cells increased from very few in the absence to about 70% in the presence of antigenic peptide, inhibition of NAADP signalling reduced the percentage down to 44%, thereby partially reverting antigenic stimulation.

Several aspects of the NAADP signalling pathway have been analysed in T cells. In the CD4+ T-lymphoma cell line Jurkat, TCR/CD3 ligation evoked a biphasic increase in NAADP, consisting of a rapid and high rise within the first 10 to 20 sec followed by a much smaller and slower increase over the next minutes (Gasser et al., 2006). Upon microinjection into Jurkat T cells, NAADP stimulated Ca^{2+} signalling with a bell-shaped concentration-response curve (Berg et al., 2000). Both initial local as well as global Ca^{2+} signals observed upon NAADP administration were sensitive to gene silencing of ryanodine receptors (Langhorst et al., 2004; Dammermann and Guse, 2005). Unexpectedly, evidence for involvement of acidic Ca^{2+} stores in NAADP signalling was not obtained in CD4+ Jurkat T cells,[45] though a recent paper reported Ca^{2+} release from acidic cytolytic granules of CD8+

T cells (Davis et al., 2012). In rat CD4+ effector T cells NAADP signalling turned out to be a major player in the cellular activation process, likely by delivering trigger Ca^{2+} that acts as co-agonist at IP_3R and RyR (Dammermann et al., 2009). This finding was confirmed in a transfer experimental autoimmune encephalomyelitis (EAE) rat model, often used to mimic aspects of the human disease multiple sclerosis. Cordiglieri et al., showed that treatment of rats with NAADP antagonist BZ194 interfered with movements of effector T cells towards the central nervous system and decreased re-activation of MBP specific CD4+ effector T cells in the brain (Cordiglieri et al., 2010). Importantly, several control experiments in whole animals or rat T cells indicate no obvious side effects of BZ194 suggesting sufficient specificity of the antagonist. Taken, together NAADP signalling plays a pivotal role for activation of CD4+ T cells. Rapid formation of endogenous NAADP and immediate local Ca^{2+} signalling upon NAADP microinjection are compatible with the idea that NAADP provides the first increase in $[Ca^{2+}]_i$ that is used then to enhance CICR via IP_3R and RyR.

IS formation occurred as soon as $[Ca^{2+}]_i$ increased, visible as rapid cellular rounding and the stop of cell motility in our experiments, as demonstrated in Donnadieu et al. (1994). Reorganization of the actin cytoskeleton is a hallmark of IS formation. Signalling proteins involved in this process are the Rho family GTPases Rac1 and Cdc42, and downstream of Cdc42 the Wiskott-Aldrich syndrome protein WASp (Badour et al., 2003). Moreover, downstream of Rac1 WAVE2 and WAVE2 complex proteins, such as Abi-2 and HEM-1, appear important for actin reorganisation since WAVE2 co-localized to IS (Nolz et al., 2006). Furthermore, gene silencing of WAVE2 and HEM-1 reduced the number of cell–cell conjugate formation (Nolz et al., 2006). Moreover, it was demonstrated that under control conditions, Jurkat T cells formed a ring-like lamellipodal interface composed of F-actin on OKT3-coated surface within 1.5 min; upon gene silencing of WAVE2, these ring-like lamellipodal interfaces were not observed resulting in lack of spreading of T cells on the OKT3-coated surface (Nolz et al., 2006). Kaizuka et al., elegantly tracked movements of TCR, ICAM-1 and actin filaments during the process of IS formation (Kaizuka et al., 2007). Importantly, they showed that in IS-forming Jurkat T cells actin speckles moved from peripheral lamella towards the IS in a directed fashion, forming a ring of actin filaments around the central supramolecular activation cluster (cSMAC). Under these conditions, the retrograde flow of actin typical for moving cells was stopped. Instead, T cells used the actin cytoskeleton for cSMAC and peripheral supramolecular activation cluster (pSMAC) formation. Microclusters composed of TCR and ICAM-1 move along underlying cytoskeleton towards the synapse to form cSMAC and pSMAC, though at slower velocity.[37] This shift of actin cytoskeleton action was determined as decreasing cell shape index in our experiments. Since in our experiments NAADP antagonist BZ194 prevented cell rounding and stop of motility, NAADP mediated initiation of Ca^{2+} signalling appears a central step in remodelling of the actin cytoskeleton. Although ring-like lamellipodal interfaces were formed rapidly after TCR/CD3 engagement (within 1.5 min; Nolz et al., 2006), we described an even faster biochemical signalling event, the formation of NAADP within 10 to 20 sec upon anti-CD3 mAb stimulation (Gasser et al., 2006). Based on our experimental data, we cannot distinguish whether NAADP evoked, and initially localized Ca^{2+} release would be sufficient to shift actin cytoskeletal function from motility to IS formation, or whether NAADP evoked Ca^{2+} release is simply necessary to provide a sufficiently high Ca^{2+} signal

via IP_3R and/or RyR to induce the shift in actin cytoskeletal function. However, our data indicate a pivotal role of NAADP signalling for IS formation and thus for activation of CD4+ T cells in general.

Acknowledgments

This work was supported by the Deutsche Forschungsgemeinschaft (grant no GU360/15-1 to AHG; FL 377/2-1 and FOR1336 to AF) and by the Wellcome Trust (Biomedical Research Collaboration Grant 068065 to BVLP and AHG). BVLP is a Wellcome Trust Senior Investigator (grant 101010).

Abbreviations

APC	antigen presenting cell
$[Ca^{2+}]_i$	free cytosolic Ca^{2+} concentration
cADPR	cyclic ADP-ribose
CICR	Ca^{2+}-induced Ca^{2+}-release
c(p)SMAC	central (peripheral) supramolecular activation cluster
IP_3	D-*myo*-inositol 1,4,5-trisphosphate
IP_3R	D-*myo*-inositol 1,4,5-trisphosphate receptor
IS	immune synapse
MBP	myelin basic protein
NAADP	nicotinic acid adenine dinucleotide phosphate 3
TCR/CD3	T cell receptor/CD3-complex
T_{MBP}	cells, MBP-specific T cells

References

Aarhus R, Graeff RM, Dickey DM, Walseth TF, Lee HC. ADP-ribosyl cyclase and CD38 catalyze the synthesis of a calcium-mobilizing metabolite from NADP. J Biol Chem. 1995; 270:30327–30333. [PubMed: 8530456]

Badour K, Zhang J, Shi F, McGavin MK, Rampersad V, Hardy LA, Field D, Siminovitch KA. The Wiskott-Aldrich syndrome protein acts downstream of CD2 and the CD2AP and PSTPIP1 adaptors to promote formation of the immunological synapse. Immunity. 2003; 18:141–154. [PubMed: 12530983]

Barceló-Torns M, Lewis AM, Gubern A, Barneda D, Bloor-Young D, Picatoste F, Churchill GC, Claro E, Masgrau R. NAADP mediates ATP-induced Ca^{2+} signals in astrocytes. FEBS Lett. 2011; 585:2300–2306. [PubMed: 21664355]

Berg I, Potter BV, Mayr GW, Guse AH. Nicotinic acid adenine dinucleotide phosphate (NAADP+) is an essential regulator of T-lymphocyte Ca^{2+}-signaling. J Cell Biol. 2000; 150:581–8. [PubMed: 10931869]

Brailoiu E, Churamani D, Cai X, Schrlau MG, Brailoiu GC, Gao X, Hooper R, Boulware MJ, Dun NJ, Marchant JS, Patel S. Essential requirement for two-pore channel 1 in NAADP-mediated calcium signaling. J Cell Biol. 2009; 186:201–209. [PubMed: 19620632]

Europe PMC Funders Author Manuscripts

Calcraft PJ, Ruas M, Pan Z, Cheng X, Arredouani A, Hao X, Tang J, Rietdorf K, Teboul L, Chuang KT, Lin P, et al. NAADP mobilizes calcium from acidic organelles through two-pore channels. Nature. 2009; 459:596–600. [PubMed: 19387438]

Cordiglieri C, Odoardi F, Zhang B, Nebel M, Kawakami N, Klinkert WE, Lodygin D, Lühder F, Breunig E, Schild D, Ulaganathan VK, et al. Nicotinic acid adenine dinucleotide phosphate-mediated calcium signalling in effector T cells regulates autoimmunity of the central nervous system. Brain. 2010; 133:1930–1943. [PubMed: 20519328]

Cosker F, Cheviron N, Yamasaki M, Menteyne A, Lund FE, Moutin MJ, Galione A, Cancela JM. The ecto-enzyme CD38 is a nicotinic acid adenine dinucleotide phosphate (NAADP) synthase that couples receptor activation to Ca^{2+} mobilization from lysosomes in pancreatic acinar cells. J Biol Chem. 2010; 285:38251–38259. [PubMed: 20870729]

Dammermann W, Guse AH. Functional ryanodine receptor expression is required for NAADP-mediated local Ca^{2+} signaling in T-lymphocytes. J Biol Chem. 2005; 280:21394–21399. [PubMed: 15774471]

Dammermann W, Zhang B, Nebel M, Cordiglieri C, Odoardi F, Kirchberger T, Kawakami N, Dowden J, Schmid F, Dornmair K, Hohenegger M, et al. NAADP-mediated Ca^{2+} signaling via type 1 ryanodine receptor in T cells revealed by a synthetic NAADP antagonist. Proc Natl Acad Sci USA. 2009; 106:10678–83. [PubMed: 19541638]

Davis LC, Morgan AJ, Chen JL, Snead CM, Bloor-Young D, Shenderov E, Stanton-Humphreys MN, Conway SJ, Churchill GC, Parrington J, Cerundolo V, et al. NAADP Activates Two-Pore Channels on T Cell Cytolytic Granules to Stimulate Exocytosis and Killing. Curr Biol. 2012; pii: S0960-9822(12)01256-0, Epub ahead of print. doi: 10.1016/j.cub.2012.10.035

Donnadieu E, Bismuth G, Trautmann A. Antigen recognition by helper T cells elicits a sequence of distinct changes of their shape and intracellular calcium. Curr Biol. 1994; 4:584–595. [PubMed: 7953532]

Eylar EH, Jackson JJ, Kniskern PJ. Suppression and reversal of allergic encephalomyelitis in rhesus monkeys with basic protein and peptides. Neurochem Res. 1979; 4:249–58. [PubMed: 88679]

Flügel A, Willem M, Berkowicz T, Wekerle H. Gene transfer into CD4+ T lymphocytes: Green fluorescent protein-engineered, encephalitogenic T cells illuminate brain autoimmune responses. Nat Med. 1999; 5:843–7. [PubMed: 10395334]

Gasser A, Bruhn S, Guse AH. Second messenger function of nicotinic acid adenine dinucleotide phosphate revealed by an improved enzymatic cycling assay. J Biol Chem. 2006; 281:16906–13. [PubMed: 16627475]

Gerasimenko JV, Maruyama Y, Yano K, Dolman NJ, Tepikin AV, Petersen OH, Gerasimenko OV. NAADP mobilizes Ca^{2+} from a thapsigargin-sensitive store in the nuclear envelope by activating ryanodine receptors. J Cell Biol. 2003; 163:271–82. [PubMed: 14568993]

Gerasimenko JV, Sherwood M, Tepikin AV, Petersen OH, Gerasimenko OV. NAADP, cADPR and IP_3 all release Ca^{2+} from the endoplasmic reticulum and an acidic store in the secretory granule area. J Cell Sci. 2006; 119:226–38. [PubMed: 16410548]

Guse AH, Goldwich A, Weber K, Mayr GW. Non-radioactive, isomer-specific inositol phosphate mass determinations: high-performance liquid chromatography-micro-metal-dye detection strongly improves speed and sensitivity of analyses from cells and micro-enzyme assays. J Chromatogr B Biomed Appl. 1995; 672:189–198. [PubMed: 8581124]

Guse AH. Linking NAADP to ion channel activity: A unifying hypothesis. Sci Signal. 2012; 5:pe18. [PubMed: 22534131]

Guse AH, Lee HC. NAADP: a universal Ca^{2+} trigger. Sci Signal. 2008; 1:re10. [PubMed: 18984909]

Guse AH, Roth E, Emmrich F. Intracellular Ca^{2+} pools in Jurkat T-lymphocytes. Biochem J. 1993; 291:447–51. [PubMed: 8484725]

Guse AH, da Silva CP, Berg I, Skapenko AL, Weber K, Heyer P, Hohenegger M, Ashamu GA, Schulze-Koops H, Potter V, Mayr GW. Regulation of calcium signalling in T lymphocytes by the second messenger cyclic ADP-ribose. Nature. 1999; 398:70–73. [PubMed: 10078531]

Hohenegger M, Suko J, Gscheidlinger R, Drobny H, Zidar A. Nicotinic acid-adenine dinucleotide phosphate activates the skeletal muscle ryanodine receptor. Biochem J. 2002; 367:423–431. [PubMed: 12102654]

Kaizuka Y, Douglass AD, Varma R, Dustin ML, Vale RD. Mechanisms for segregating T cell receptor and adhesion molecules during immunological synapse formation in Jurkat T cells. Proc Natl Acad Sci USA. 2007; 104:20296–20301. [PubMed: 18077330]

Kim B, Park K, Yim C, Takasawa S, Okamoto H, Im M, Kim U. Generation of nicotinic acid adenine dinucleotide phosphate and cyclic ADP-ribose by glucagon-like peptide-1 evokes Ca^{2+} signal that is essential for insulin secretion in mouse pancreatic islets. Diabetes. 2008; 57:868–78. [PubMed: 18184929]

Krummel MF, Cahalan MD. The immunological synapse: A dynamic platform for local signaling. J Clin Immunol. 2010; 30:364–372. [PubMed: 20390326]

Kunerth S, Mayr GW, Koch-Nolte F, Guse AH. Analysis of subcellular calcium signals in T-lymphocytes. Cell Signal. 2003; 15:783–92. [PubMed: 12781871]

Kunerth S, Langhorst MF, Schwarzmann N, Gu X, Huang L, Yang Z, Zhang L, Mills SJ, Zhang L, Potter BVL, Guse AH. Amplification and propagation of pacemaker Ca^{2+} signals by cyclic ADP-ribose and the type 3 ryanodine receptor in T cells. J Cell Sci. 2004; 117:2141–2149. [PubMed: 15054112]

Langhorst MF, Schwarzmann N, Guse AH. Ca^{2+} release via ryanodine receptors and Ca^{2+} entry: Major mechanisms in NAADP-mediated Ca^{2+} signaling in T-lymphocytes. Cell Signal. 2004; 16:1283–9. [PubMed: 15337527]

Lee HC. Cyclic ADP-ribose and nicotinic acid adenine dinucleotide phosphate (NAADP) as messengers for calcium mobilization. J Biol Chem. 2012; 287:31633–31640. [PubMed: 22822066]

Lee HC. The cyclic ADP-Ribose/NAADP/CD38-signaling pathway: Past and present. Messenger. 2012; 1:16–33.

Lee HC, Aarhus R. A derivative of NADP mobilizes calcium stores insensitive to inositol trisphosphate and cyclic ADP-ribose. J Biol Chem. 1995; 270:2152–2157. [PubMed: 7836444]

Lewis AM, Aley PK, Roomi A, Thomas JM, Masgrau R, Garnham C, Shipman K, Paramore C, Bloor-Young D, Sanders LE, Terrar DA, et al. ß-Adrenergic receptor signaling increases NAADP and cADPR levels in the heart. Biochem Biophys Res Commun. 2012; 427:326–329. [PubMed: 22995315]

Lin-Moshier Y, Walseth TF, Churamani D, Davidson SM, Slama JT, Hooper R, Brailoiu E, Patel S, Marchant JS. Photoaffinity labeling of nicotinic acid adenine dinucleotide phosphate (NAADP) targets in mammalian cells. J Biol Chem. 2012; 287:2296–2307. [PubMed: 22117075]

Masgrau R, Churchill GC, Morgan AJ, Ashcroft SJ, Galione A. NAADP: a new second messenger for glucose-induced Ca^{2+} responses in clonal pancreatic beta cells. Curr Biol. 2003; 13:247–251. [PubMed: 12573222]

Mojzisová A, Krizanová O, Záciková L, Komínková V, Ondrias K. Effect of nicotinic acid adenine dinucleotide phosphate on ryanodine calcium release channel in heart. Pflugers Arch. 2001; 441:674–677. [PubMed: 11294249]

Morgan AJ, Platt FM, Lloyd-Evans E, Galione A. Molecular mechanisms of endolysosomal Ca^{2+} signalling in health and disease. Biochem J. 2011; 439:349–374. [PubMed: 21992097]

Nolz JC, Gomez TS, Zhu P, Li S, Medeiros RB, Shimizu Y, Burkhardt JK, Freedman BD, Billadeau DD. The WAVE2 complex regulates actin cytoskeletal reorganization and CRAC-mediated calcium entry during T cell activation. Curr Biol. 2006; 16:24–34. [PubMed: 16401421]

Ogunbayo OA, Zhu Y, Rossi D, Sorrentino V, Ma J, Zhu MX, Evans AM. Cyclic adenosine diphosphate ribose activates ryanodine receptors, whereas NAADP activates two-pore domain channels. J Biol Chem. 2011; 286:9136–9140. [PubMed: 21216967]

Schmid F, Bruhn S, Weber K, Mittrücker HW, Guse AH. CD38: A NAADP degrading enzyme. FEBS Lett. 2011; 585:3544–3548. [PubMed: 22020217]

Soares S, Thompson M, White T, Isbell A, Yamasaki M, Prakash Y, Lund FE, Galione A, Chini EN. NAADP as a second messenger: Neither CD38 nor base-exchange reaction are necessary for in vivo generation of NAADP in myometrial cells. Am J Physiol Cell Physiol. 2007; 292:C227–239. [PubMed: 16790499]

Steen M, Kirchberger T, Guse AH. NAADP mobilizes calcium from the endoplasmic reticular Ca^{2+} store in T-lymphocytes. J Biol Chem. 2007; 282:18864–71. [PubMed: 17446167]

Walseth TF, Lin-Moshier Y, Weber K, Marchant JS, Slama JT, Guse AH. Nicotinic acid adenine dinucleotide 2'-phosphate (NAADP) binding proteins in T-lymphocytes. Messenger. 2012; 1:86–94. [PubMed: 24829846]

Wang X, Zhang X, Dong XP, Samie M, Li X, Cheng X, Goschka A, Shen D, Zhou Y, Harlow J, Zhu MX, et al. TPC proteins are phosphoinositide- activated sodium-selective ion channels in endosomes and lysosomes. Cell. 2012; 151:372–383. [PubMed: 23063126]

Yamaguchi S, Jha A, Li Q, Soyombo AA, Dickinson GD, Churamani D, Brailoiu E, Patel S, Muallem S. Transient receptor potential mucolipin 1 (TRPML1) and two-pore channels are functionally independent organellar ion channels. J Biol Chem. 2011; 286:22934–22942. [PubMed: 21540176]

Yamasaki M, Thomas JM, Churchill GC, Garnham C, Lewis AM, Cancela JM, Patel S, Galione A. Role of NAADP and cADPR in the induction and maintenance of agonist-evoked Ca^{2+} spiking in mouse pancreatic acinar cells. Curr Biol. 2005; 15:874–878. [PubMed: 15886108]

Zhang F, Li P. Reconstitution and characterization of a nicotinic acid adenine dinucleotide phosphate (NAADP)-sensitive Ca^{2+} release channel from liver lysosomes of rats. J Biol Chem. 2007; 282:25259–69. [PubMed: 17613490]

Zhang F, Jin S, Yi F, Li P. TRP-ML1 functions as a lysosomal NAADP-sensitive Ca^{2+} release channel in coronary arterial myocytes. J Cell Mol Med. 2009; 13:3174–85. [PubMed: 18754814]

Europe PMC Funders Author Manuscripts

Europe PMC Funders Author Manuscripts

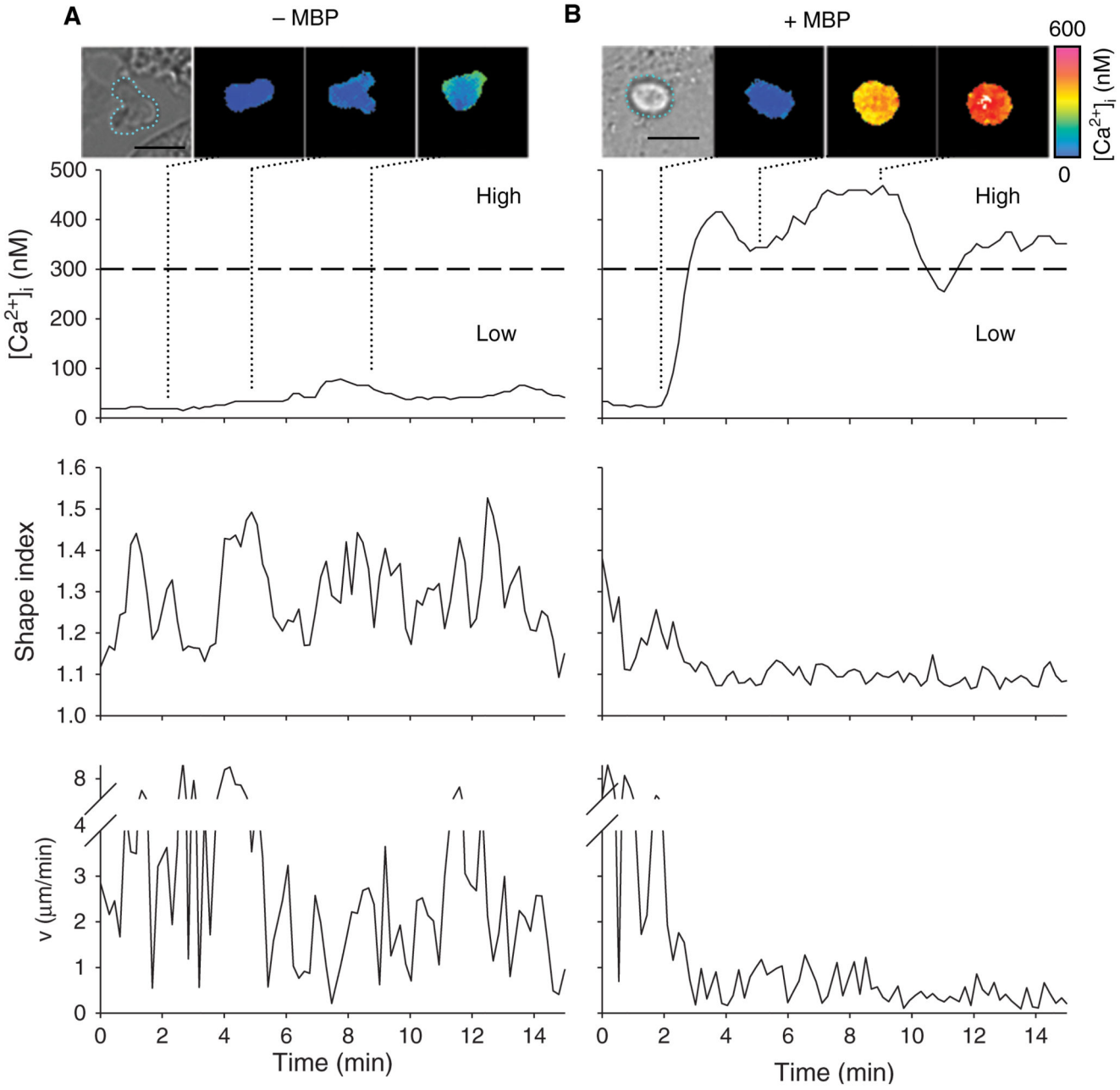

Figure 1.

Ca^{2+} signalling, shape index and motility of T_{MBP} cells during immune synapse formation. Astrocytes were pulsed (A) or not (B) with MBP. Resting rat T_{MBP} cells were added to the astrocytes and Ca^{2+}-signalling, shape index and motility were analysed. Top: Transmitted light and colour-coded images showing single cell analyses of representative T cells. T cells are highlighted by green lines in the transmitted light images. Length scale = 10 μm. Quantification of $[Ca^{2+}]_i$, changes in shape index and motility in the first 15 minutes after contact to an astrocyte are shown in the panels below.

Europe PMC Funders Author Manuscripts

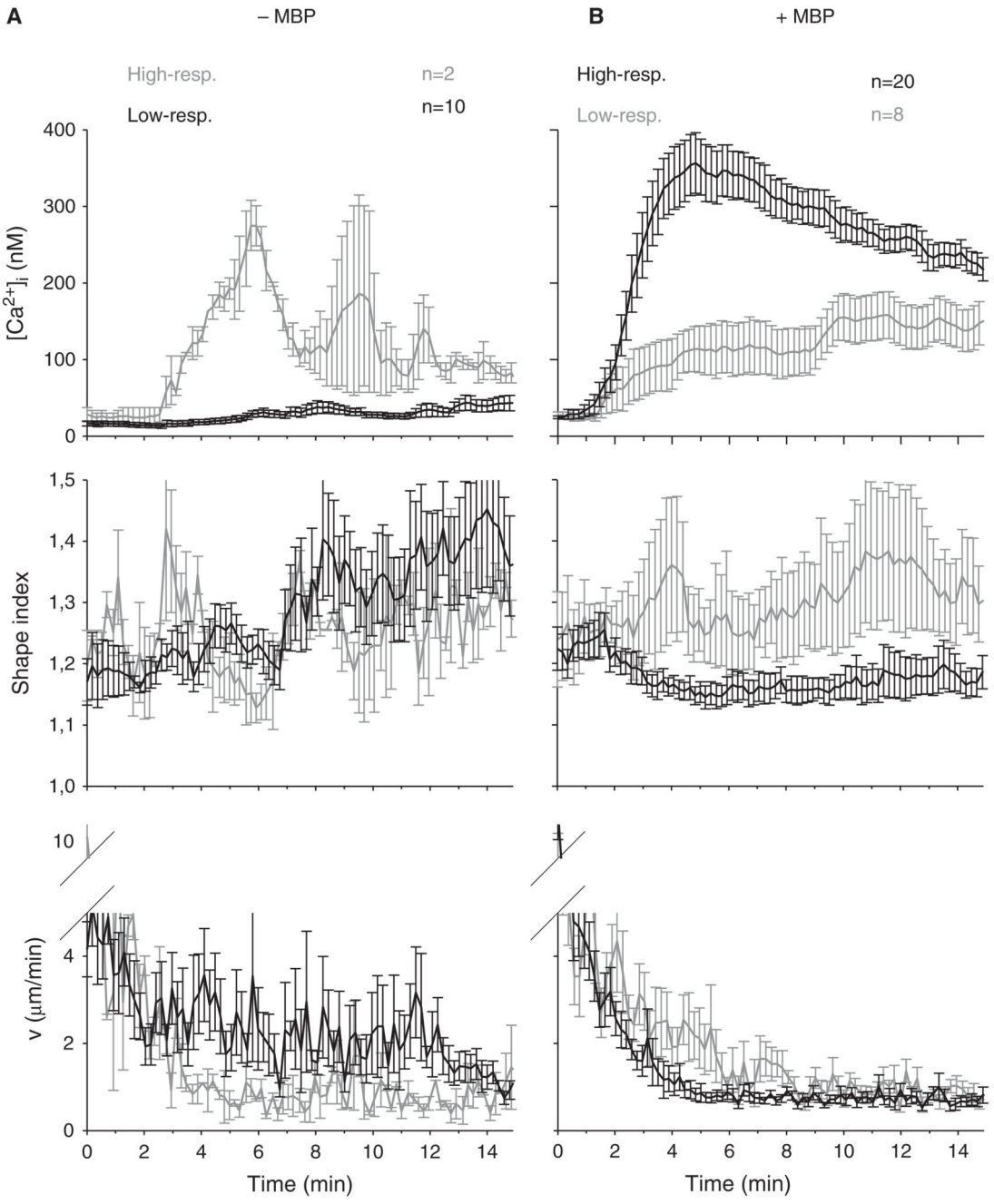

Figure 2.

Ca^{2+} signalling, shape and motility pattern of high- and low-responding T_{MBP} cells. Mean $[Ca^{2+}]_i$, shape index and motility of T_{MBP} cells after contact to MBP-pulsed (right) astrocytes are displayed (±SEM). Control T cells with non-pulsed astrocytes are shown on the left. Black lines correspond to the majority and grey lines to the minority of T cells at a certain condition (+/− MBP).

Europe PMC Funders Author Manuscripts

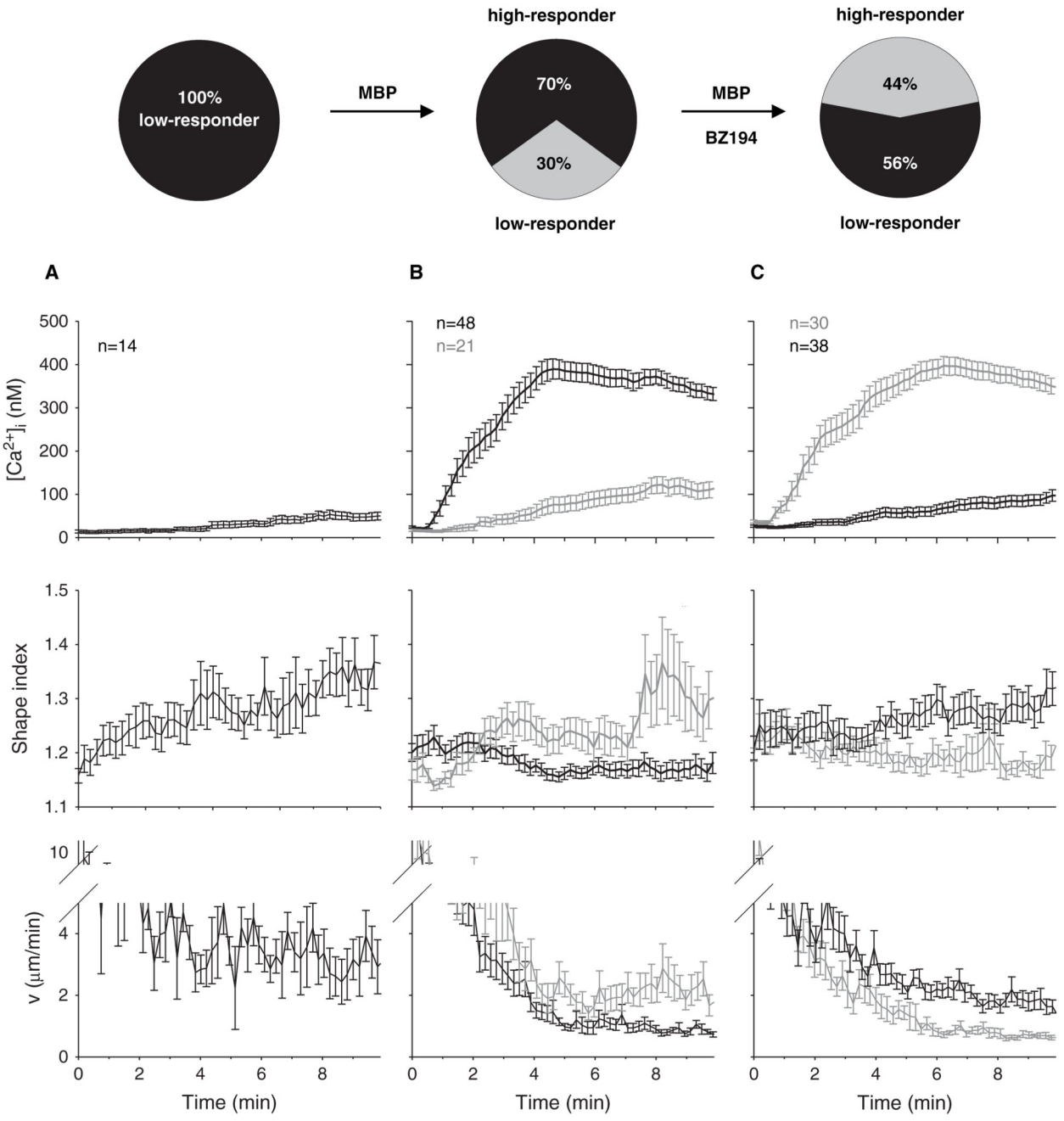

Figure 3.

NAADP-antagonist BZ194 inhibits Ca^{2+}-signalling and immune synapse formation in T_{MBP} cells stimulated by MBP-pulsed astrocytes. Astrocytes with were pulsed with MBP. Resting rat T_{MBP} cells were incubated with BZ194 (C) or left untreated (B). In control experiments astrocytes were not pulsed with MBP (A). T cells were added to the astrocytes and Ca^{2+}-signalling was measured. Top: Percentage of T cells showing Ca^{2+}-signals above (high-responders) or below (low-responders) 300 nM $[Ca^{2+}]_i$ in the first ten minutes after contact to an astrocyte. Bottom: Averaged tracings (±SEM) of T cells showing kinetics of $[Ca^{2+}]_i$,

changes in shape index and motility in the first ten minutes after contact to an astrocyte. The majority of T cells is displayed in black, the minority in grey.

Europe PMC Funders Author Manuscripts